2011 American Control Conference
on O'Farrell Street, San Francisco, CA, USA
June 29 - July 01, 2011

Robust Adaptive Control of a Magnetic Shape Memory Actuator for Precise Positioning

Leonardo Riccardi, David Naso, Biagio Turchiano, Hartmut Janocha

***Abstract*—Due to their outstanding strain capability, Magnetic Shape Memory actuators are a promising technology for positioning systems. Their wide hysteresis and dependence on temperature require a control system capable to cope with time-varying hysteresis as well as other uncertainties. In this paper, we adopt a modified Prandtl-Ishlinskii operator to capture and compensate by inverse model the hysteresis adaptively. A robust adaptive controller based on adaptive bounding techniques is then designed and integrated in order to improve the performance of the adaptive compensator. Experimental results on a 1DOF linear positioning prototype with micrometric precision confirm the effectiveness of the approach.**

I. Introduction

In different application fields, ranging from bioengineering to aerospace robotics, the ever wide use of *smart materials*, which include the well-known piezoelectric or magnetostrictive materials as well as the younger and less studied magnetic shape memory alloys (MSMA), permits to extend the engineering standards in terms of accuracy, efficiency and lightness [1]. In particular, MSMA belong to a new interesting category of active materials for their outstanding strain capability (more than one order of magnitude larger than piezoelectric materials) and the possibility to control it by excitation with a magnetic field [2], [3].

The remarkable, magnetically-induced strain exhibited by the MSMA make them particularly suitable for the development of new compact positioning system. However, two main drawbacks must be faced when dealing with these alloys, namely, the wide hysteresis between the input (field or current) and the mechanical output (strain), representing the *quasi-static*, *rate-independent* memory behaviour caused by energy losses, and the strong influence of the temperature on material behavior. Considering the characteristic of MSMA available to date (the internal temperature rapidly raises with the frequency of the magnetic excitation due to internal friction forces), any application intended to fully exploit the potentials of the material has to be equipped with some *adaptive hysteresis compensation* strategy [4].

Adaptive hysteresis compensation requires a model of the hysteresis to be identified and used in real-time. Literature offers a wide choice of phenomenological models, such as Prandtl-Ishlinskii model (PIM) [5], which has the important feature of an analytically computable inverse model. An adaptive version of the PIM has been developed in [6]. Since the PIM cannot describe asymmetric hysteresis loops, generalized [7] and non-symmetric [8] PIM have been proposed. Such references, as well as several other related contributions ([9], [10], [11]), use the direct hysteresis model to achieve a high-performing stable closed loop control without the need of computing its inverse. In this paper, we investigate and revisit a different, more "classical" direction for hysteresis compensation based on inverse models. Indeed, the proposed approach is a combination of several effective tools for dealing with practical issues related to adaptive control. The considered scheme is based on an inverse modified PIM (MPIM) whose parameters are adapted on line. The MPIM is generated by the composition of a *memory operator* and a *memoryless operator* and is capable of modeling asymmetrical hysteresis. The method permits a simplified description of the control loop, which in turn allows us to obtain models with a smaller number of parameters if compared to other available approaches. Stability and robustness to uncertainties are achieved with a further component of the controller based on adaptive bounding in presence of actuator saturation. This issue, often neglected when dealing with hysteresis on piezoelectric actuators [12], [13], is particularly crucial in our magnetically-driven equipment due to both current amplification and magnetic circuit inherent saturation limits.

The overall control loop is experimentally tested on a prototype of 1DOF precise positioning system subject to external disturbances, and a comparison with other approaches described in literature is provided.

The paper is organized ad follows. Section II introduces the MPIM while section III introduces the actuator under analysis and illustrates the robust controller design with a discussion of closed loop stability. Finally Section IV and V provide discussion of the experimental result and some conclusive remarks.

Manuscript received September 22, 2010. This work was partially funded by Regione Puglia, A.Q.P. Ricerca, Progetto "Modelli Innovativi per Sistemi Meccatronici", Del. CIPE 20/04, DM01, and by the DFG (German Research Foundation), SPP 1239/B9.

L. Riccardi, D. Naso, B. Turchiano are with Department of Electronics and Electrical Science (DEE) at the Politecnico di Bari, Bari, Italy. (mail: riccardi@deemail.poliba.it).

H. Janocha is with the Laboratory of Process Automation (LPA) at Saarland University, Saarbruecken, Germany. (mail: janocha@lpa.uni-saarland.de).

II. The Modified Prandtl-Ishlinskii Model

In this section we introduce the *modified Prandtl-Ishlinskii model* (MPIM) for hysteretic nonlinearities. As the main ideas and notation are derived from the work in [14] and [15], we will limit our attention to the essential concepts. The overall model is composed of the simple Prandtl-Ishlinskii model (PIM) and the superposition operator (SO), described in the following subsection. The remaining part of the section will be dedicated to compensation and identification strategies.

A. The modified Prandtl-Ishlinskii hysteresis operator

Essentially, the MPIM is the cascade of a standard PIM and a memory-free, piecewise linear, parameterized scalar function, called threshold-discrete Prandtl-Ishlinskii Superposition Operator (SO for brevity). The PIM describes a complex hysteresis as the weighted superposition of *N+1* elementary (backlash or play) operators called *hysterons* (each defined by a single threshold parameter), where *N* is called the *order* of the PIM. In a compact notation, the PIM can be expressed as:

$$v = H[i] = \sum_{j=0}^{N} p_j H_j\left[i; r_j\right] = \underline{p}^T \underline{H}\left[i; \underline{r}\right], \tag{1}$$

with $\underline{p} = \left(p_0..p_j..p_N\right)^T$ is the vector of weights, $\underline{H}[i] = \left(H_0[i]..H_j[i]..H_N[i]\right)^T$ is the vector of the elementary operators and $\underline{r}$ is the vector of thresholds.

To overcome the approximation limits of the standard PI model, reference [8] proposes to add a piecewise linear scalar function (called *Superposition Operator*, SO) obtained as the weighted sum of the so-called elementary *one-sided dead-zone operators* (DZO) in series with the PIM. The generic *l-th* DZO depends only on its threshold a_l. The output *x* of the SO is:

$$x = S(v) = \sum_{l=-L}^{L} w_l S_l\left(v; a_l\right) = \underline{w}^T \underline{S}\left(v; \underline{a}\right), \tag{2}$$

In (2) it is assumed that the elementary operators are organized in a vector $\underline{S}$ so that the thresholds (also organized in a vector $\underline{a}$) form an ordered sequence $a_{-L} < .. < a_0 = 0 < .. < a_L$. As a consequence, the SO has *2L+1* elementary operators, where *L* is called the *order* of the SO. To simplify the notation, hereafter we will drop the dependence from the thresholds. Thus, the modified PI model Γ (MPIM) is defined as the series between the PIM and the SO, i.e.,

$$x = \Gamma[i] = \underline{w}^T \underline{S}\left(\underline{p}^T \underline{H}[i]\right). \tag{3}$$

As discussed in [8], the inverse MPIM Γ^{-1} (IMPIM) can be computed analytically as the series between the Inverse SO (ISO) and the Inverse PI (IPI), i.e.,

$$i = \Gamma^{-1}[x] = \underline{p}_I^T \underline{H}_I\left[\underline{w}_I^T \underline{S}_I(x)\right]. \tag{4}$$

The inversion obviously requires that both PIM and SO are invertible, a circumstance that occurs if and only if the weights $\underline{p}$ and $\underline{w}$ satisfy some inequality constraints [14] related to monotonicity properties. Note that the IPI and ISO have the same structure of their direct counterparts, but their weights and thresholds are different. There is a unique, direct mapping between the weights and thresholds of the MPIM and the corresponding weights and thresholds of the IMPIM. If the firsts are available, the others can be readily calculated.

B. Off-line and on-line identification

The thresholds $\underline{r}$ and $\underline{a}_I$ can be determined *a priori* based on the amplitudes of the input and output signals, for example with a uniform distribution over the entire signals range. The identification of the MPIM relies on the identification of the weights $\underline{w}_I$ and $\underline{p}$. Both off-line and on-line identifications are carried out as the *constrained minimization* of the L_2-norm of the following error:

$$e\left(\underline{p}, \underline{w}\right) = \underline{p}^T \underline{H}[i] - \underline{w}_I^T \underline{S}_I[x] \tag{5}$$

The minimization provides us with $\underline{p}$ and $\underline{w}_I$ or, if adaptive, with their estimates. $\hat{\underline{p}}$ and $\hat{\underline{w}}_I$. The interested reader can refer to [6] and [15] for a detailed treatment of the topic.

III. Robust Control Design For Precise Positioning

The adaptive MPIM is able to capture the hysteresis phenomenon inside the actuator with a precision that increases with the order of the model, until a given limit is reached. In fact, as in all adaptive approaches, the performance of the compensation is not only limited by the minimum functional approximation error (MFAE) of the model, but significantly affected by disturbance and other unmodeled dynamics, especially in practical applications. Finding an adequate tradeoff between the complexity of the approximator (number of parameters), the actual asymptotical performance (the residual tracking error when the parameter have converged) and disturbance rejection is a well-known control engineering problem requiring nontrivial design and tuning efforts in most practical applications. In this paper, the problem is addressed with an additional control loop taking care of imperfect hysteresis compensation and additional performance improvements. Before discussing the control design, in the following we briefly present the actuator and its characteristics.

A. The MSM positioning actuator

The actuator (see Fig. 1) is composed by three main parts: the magnetic circuit, made by the excitation coils and the flux guide that provides the magnetic field *H* to the element; the MSMA element, that is the coupling between the

magnetic part and the mechanical part; the mechanical part, composed by a push rod that provides the interface of the device with the external world.

The actuator is located in the middle of a platform that comprehends a position sensor on the top, a Hall probe to measure the flux density and a current amplifier that provides the control signal (further details on the hardware can be found in [4]). The goal of the actuator and the control loop is to produce a desired motion in the vertical direction (*x*-axis). Fig. 2 shows the characteristics between the driving current *i*, the magnetic flux density *B* in the actuator and the displacement *x,* in the chosen working range with $i(t) \in [0, 2.2]$ A, emphasizing the presence of a strong asymmetric hysteresis (dependence of this curve from temperature is also reported in [4]).

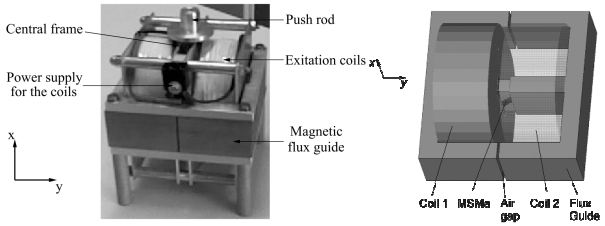

Fig. 1. MSMA actuator and its simplified functional scheme

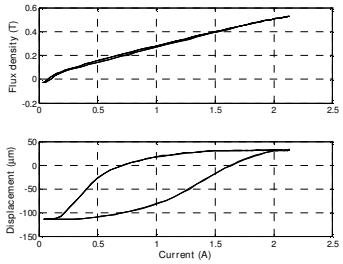

Fig. 2. Characteristics of the actuator in the working range

B. General overview of the controlled plant

We consider the description of the plant shown in Fig. 3. The plant to be controlled is composed by the MSMA actuator in series with a voltage-controlled current source (current amplifier). The MSMA actuator does not posses a visible dynamics. Hysteresis is its main phenomenon and is taken into account by the operator Γ.

The current amplifier, instead, is characterized by a cut-off frequency f_{CUT} of about 20 Hz and saturation between 0 and 2.2 A. It can be represented in the Laplace domain by a first-order dynamic filter $A(s)$, where s is the Laplace variable. The symbol i^* indicates the current requested from the control board whereas i is the current that flows in the excitation circuit of the actuator. The current i^* is the output of an adaptive hysteresis compensator $\hat{\Gamma}^{-1}$, $i^* = \hat{\Gamma}^{-1}[v]$ where v is the saturated control action (we consider the saturation of the amplifier inside the controller).

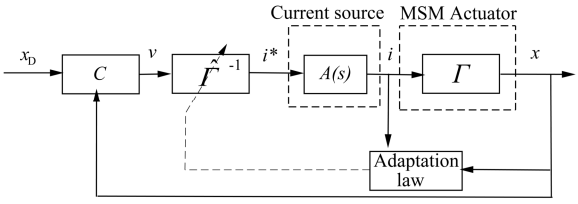

Fig. 3. Description of the plant and control loop

Obviously, the presence of the filtering $A(s)$ does not ensure the perfect compensation between v and x at all frequencies, even if the hysteresis inversion is precise (i.e. after the adaptation is completed) and $\hat{\Gamma} \to \Gamma$.

If we operate at frequencies lower than f_{CUT}, we can adopt another useful description of the system, depicted in Fig. 4.

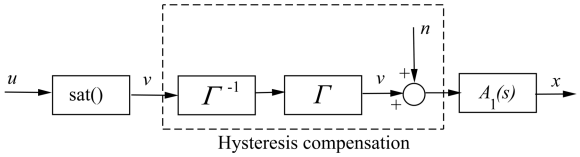

Fig. 4. Approximation of the system

The hysteresis compensation is assumed to be perfect and the modeling errors are taken into account by a disturbance contribution *n*. It is clear that *n* is big at the beginning, i.e., when the adaptation of the compensator starts, and is expected to be small at the end of the adaptation. The main difference with Fig. 3 is that a linear dynamic $A_1(s)$ with $A_1(s) \neq A(s)$ is now placed before system output. $A_1(s)$ is an approximation of the input-output dynamics of the system. In this work, based on preliminary experimental evaluations, we assume that such dynamics can be approximated by a linear model. The schema of Fig. 4 is the reference representation for the synthesis of the robust controller.

C. Controller design

We express the linear dynamics as:

$$A_1(s) = \lambda_A / (s + \lambda_A) \tag{6}$$

The parameter $\lambda_A > 0$ is considered as unknown.

The system in Fig. 4 can be expressed by the following equations.

$$\begin{cases} \dot{x} = -\lambda_A x + \lambda_A v + n \\ v = \mathrm{sat}(u) \end{cases} \tag{7}$$

with:

$$\mathrm{sat}(u) = \begin{cases} u & \text{if } u_L \le |u| \le u_U \\ (u_L & \text{if } u \le u_L) \text{ or } (u_U \text{ if } u \ge u_U) \end{cases} \tag{8}$$

We consider a desired trajectory x_D generated by an appropriate filtering of a reference signal *r*:

$$\dot{x}_D = -\hat{\lambda}_A x_D + \hat{\lambda}_A r \tag{9}$$

Eq. (9) is useful in the presence of frequency limitations on the system, because it allows to generate the desired

trajectory by a filtering of the reference with an estimation of the unknown linear dynamics ($\hat{\lambda}_A$ is an estimate of λ_A).

In order to take into account the saturation, let us consider the *support variable* z [16]:

$$\dot{z} = -\hat{\lambda}_A z + \hat{\lambda}_A (v - u) \tag{10}$$

Note that if the control variable is within the limits, then $v - u = 0$ and $z \to 0$ in a time interval depending on $\hat{\lambda}_A$. We define the modified tracking error e_M as

$$e_M = x - x_D - z \tag{11}$$

and the filtered modified tracking error as

$$e_F = e_M + k\int e_M \tag{12}$$

that corresponds to providing a proportional-integral control objective ($k \geq 0$). We notice that e_M converges to the classic tracking error $e = x - x_D$ in the case that the control action is not saturated.

Moreover, we consider that the modeling error inside the disturbance term n is bounded by unknown bounds $b_L > 0$ and $b_U > 0$, $-b_L \leq n \leq b_U \quad \forall t > 0$. The estimates of such bounds, $\hat{b}_L$ and $\hat{b}_U$, will be used to ensure the robustness of the control loop. For the system in (7) we present the following control law:

$$u = -\frac{k}{\hat{\lambda}_A} e_M - k\int e_M + r - \frac{1}{\hat{\lambda}_A}\eta(e_F) \tag{13}$$

$$\eta(e_F) = \begin{cases} -\hat{b}_L & \text{if } e_F < 0 \\ \hat{b}_U & \text{if } e_F > 0 \end{cases} \tag{14}$$

and the following adaptation laws for the parameters $\hat{b}_U$, $\hat{b}_L$, $\hat{\lambda}_A$:

$$\dot{\hat{\lambda}}_A = -\gamma_A \left(x_D + z - v - k\int e_M \right) e_F \tag{15}$$

$$\dot{\hat{b}}_L = \begin{cases} 0 & \text{if } e_F \geq 0 \\ -\gamma_b e_F & \text{if } e_F < 0 \end{cases} \tag{16}$$

$$\dot{\hat{b}}_U = \begin{cases} \gamma_b e_F & \text{if } e_F > 0 \\ 0 & \text{if } e_F \leq 0 \end{cases} \tag{17}$$

Theorem: The system described in (7), with an adaptive hysteresis compensation algorithm, the control limits in (8), the control action defined in (13) and the adaptive laws in (15), (16), (17), has all the closed loop signals bounded, and the plant output $x(t)$ follows the specified trajectory $x_D(t)$ in (9) as $t \to \infty$.

Proof. To establish the global boundedness we adopt the following Lyapunov function:

$$V = \frac{1}{2}e_F^2 + \frac{1}{2\gamma_b}\left(\tilde{b}_L\right)^2 + \frac{1}{2\gamma_b}\left(\tilde{b}_U\right)^2 + \frac{1}{2\gamma_A}\left(\tilde{\lambda}_A\right)^2 \tag{18}$$

Where $\tilde{b}_L = \hat{b}_L - b_L$, $\tilde{b}_U = \hat{b}_U - b_U$, $\tilde{\lambda}_A = \hat{\lambda}_A - \lambda_A$ and γ_b and γ_A positive constants . The derivative is:

$$\dot{V} = e_F \dot{e}_F + \frac{1}{\gamma_b}\tilde{b}_L\dot{\hat{b}}_L + \frac{1}{\gamma_b}\tilde{b}_U\dot{\hat{b}}_U + \frac{1}{\gamma_A}\tilde{\lambda}_A\dot{\hat{\lambda}}_A \tag{19}$$

Focusing on the first addendum of (24), inserting (12), (11), (9), (10) and (7) in (19) one obtains

$$e_F\dot{e}_F = e_F\left[\dot{e}_M + ke_M\right] = e_F\left[\dot{x} - \dot{x}_D - \dot{z} + ke_M\right] =$$

$$= e_F\left[-\lambda_A x + \lambda_A v + n + \hat{\lambda}_A x_D - \hat{\lambda}_A r + \hat{\lambda}_A z - \hat{\lambda}_A (v - u) + ke_M\right]$$

Then, adding and subtracting $\lambda_A x_D$, $\lambda_A z$, $\lambda_A v$ it holds

$$e_F\dot{e}_F = e_F\left[-\lambda_A e_M + \tilde{\lambda}_A (x_D + z - v) + n - \hat{\lambda}_A (r - u) + ke_M\right]$$

Adding and subtracting $\lambda_A k\int e_M$, and using (13), (19) can be rewritten as follows

$$\dot{V} = -\lambda_A e_F^2 + \tilde{\lambda}_A\left(x_D + z - v - k\int e_M\right)e_F + \left(n - \eta(e_F)\right)e_F + \frac{1}{\gamma_b}\tilde{b}_L\dot{\hat{b}}_L + \frac{1}{\gamma_b}\tilde{b}_U\dot{\hat{b}}_U + \frac{1}{\gamma_A}\tilde{\lambda}_A\dot{\hat{\lambda}}_A \tag{20}$$

Then, using (15)

$$\dot{V} = -\lambda_A e_F^2 + \left(n - \eta(e_F)\right)e_F + \frac{1}{\gamma_b}\tilde{b}_L\dot{\hat{b}}_L + \frac{1}{\gamma_b}\tilde{b}_U\dot{\hat{b}}_U \tag{21}$$

Splitting (21) in two cases, namely $e_F > 0$ and $e_F < 0$, by direct application of (14), (16) and (17) we can demonstrate that

$$\dot{V} \leq -\lambda_A e_F^2 \leq 0 \tag{22}$$

Because of (22), we can state that $e_F, \hat{b}_U, \hat{b}_L, \hat{\lambda}_A$ are uniformly bounded. Moreover, using standard arguments it can be proven that $e_F \to 0$.

Remark: the parameter $\hat{\lambda}_A$ is subjected to projection in order to ensure that $\hat{\lambda}_A > 0$.

IV. Experimental Results

This section summarizes a set of experimental results performed on the MSMA actuator with the robust adaptive hysteresis compensation (RAHC) developed in the previous section and illustrated in Fig. 3. As a reference term for comparison, we will use a standard adaptive hysteresis compensation (SAHC) strategy (such as the one described in [15]) which does not implement the external robust control loop. Both schemes use the same approximator structure with 4 PI operators and 4 superposition operators, and are initialized in the same way, having all the parameters set to zero (no a priori knowledge of the hysteresis).

A. Tracking of a sinusoidal signal

Fig. 5 shows the performance of the SAHC when tracking of a sinusoidal reference (1.5 Hz). After the initial parameter adaptation stage, which last approximately 8 s, the controller reaches a tracking error $|e| \leq 5\ \mu$m. According to our experimental investigation, this error cannot be reduced significantly by using higher order

MPIM. It may be interesting to mention that, in this specific test, Preisach-like models with larger numbers of parameters seemed to perform slightly better (a model with 49 parameters could reach errors in the range of 3 μm). Fig. 6 shows the performance of the RAHC. This controller allows the system to reach the asymptotical tracking with a nearly negligible transient and a final error $|e_M| \le 2\ \mu$m. We observed that the adaptation of parameters (not shown for space limitation) was slower than for the SAHC, and that both schemes eventually converged to almost stable values in about 15 s.

B. *Step Tracking*

Fig. 7 shows the response of SAHC for a periodic sum of steps. Although this signal is inherently unsuitable to perform hysteresis identification, it is a frequently applied type of reference in precise positioning application. The larger time needed for adaptation of the SAHC are reasonably due to nature of the reference (see [5] and [14] for discussions about this issue). Fig. 8 shows the results of the RAHC. Again, it offers a satisfactory tracking in a shorter time, disregarding the inherent limitations caused by the step signal. Fig. 8 emphasizes the contribution of the integral objective specified in (12). The overshoot, considered admissible in our test, can be regulated by properly tuning the gain k (which was left unchanged with respect to the previous test).

C. *Tracking of a sum of sinusoids with disturbance*

To test both schemes in a challenging situation, we consider the problem of tracking a sum of sinusoids between 0.5 and 2 Hz when a disturbance is acting on the position sensor. In this test, a periodic signal (a sum of sinusoids between 2 and 10 Hz) ranging in $\pm 10\ \mu$m is artificially added to the output of the sensor. Fig. 9 reports the results obtained with the SAHC. The performance of this controller is not satisfactory, as the presence of the disturbance tends to prevent the model to correctly identify the hysteresis, also limiting the performance in terms of tracking error. Fig. 10 shows the results of the RAHC. The outer loop gives a beneficial contribution also in this case, as this scheme reaches a final tracking error $|e_M| \le 5\ \mu$m against the $|e| \le 18\ \mu$m obtained by the SAHC.

V. Conclusion

In this paper we presented a control scheme with MSMA actuators. The approach combines an adaptive hysteresis compensator based on the modified Prandtl-Ishlinskii model and a robust adaptive controller which is able to improve the tracking performance of the compensator while taking into account also control saturation. At the same time, the proposed control scheme retains the advantages of standard compensation strategies relying on inverse models (simpler models with less parameters). Experimental results demonstrated the feasibility of the proposed approach. Directions for further investigations include the development of other adaptation strategies with a smaller number of configuration parameters, and new prototypes of actuators, and related controllers, with magnetically-induced (rather than mechanically-induced) contraction.

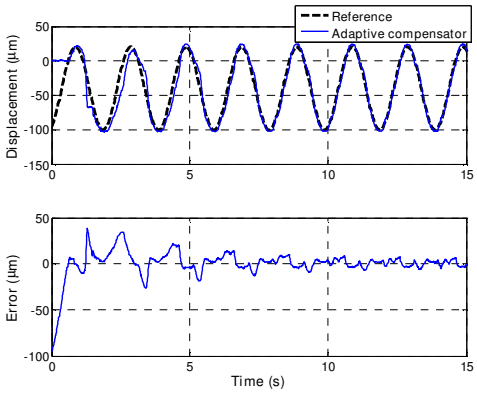

Fig. 5. Adaptive compensator for a sinus (1.5 Hz)

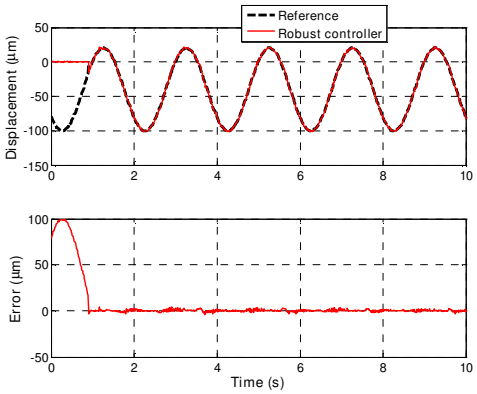

Fig. 6. Robust controller for a sinus (1.5 Hz)

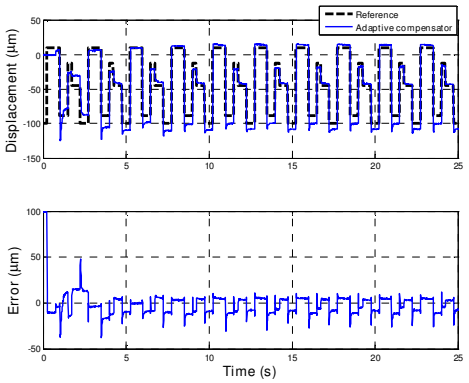

Fig. 7. Adaptive compensator for tracking of steps

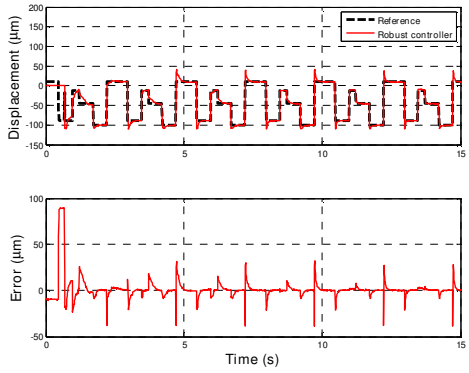

Fig. 8. Robust controller for tracking of steps

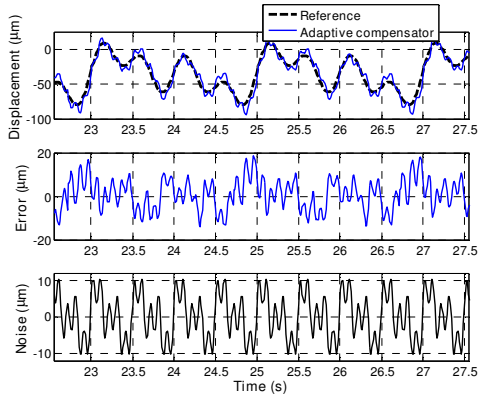

Fig. 9. Adaptive compensator for a sum of sinus with disturbance

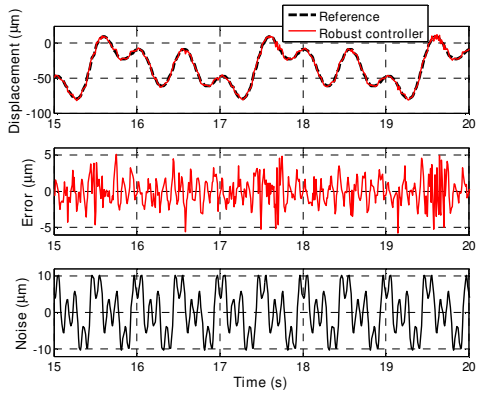

Fig. 10. Robust controller for a sum of sinus with disturbance

REFERENCES

[1] H. Janocha, *Adaptronics and Smart Structures: basics, materials, design and applications*, Springer, 2007.

[2] A. Sozinov, A. Likhachev, and K. Ullakko, "Crystal structures and magnetic anisotropy properties of Ni-Mn-Ga martensitic phases with giant magnetic-field-induced strain", *IEEE Transactions on Magnetics*, vol. 38, 2002, pp. 2814-2816.

[3] S. Faehler, "An introduction to actuation mechanisms of Magnetic Shape Memory Alloys," *ECS Transactions*, ECS, 2007, pp. 155-163.

[4] L. Riccardi, G. Ciaccia, D. Naso, H. Janocha, B. Turchiano, "Position control for a Magnetic Shape Memory actuator", *in IFAC International Symposium on Mechatronic Systems, 2010,* pp. 478 -485.

[5] P. Krejci and K. Kuhnen, "Inverse control of systems with hysteresis and creep", *IEE Proceedings-Control Theory and Applications*, vol. 148, 2001, pp. 185–192.

[6] D. Pesotski, H. Janocha, and K. Kuhnen, "Adaptive Compensation of Hysteretic and Creep Nonlinearities in Solid-State Actuators", *Journal of Intelligent Material Systems and Structures*, submitted, 2010.

[7] M. Al Janaideh, Y. Feng, S. Rakheja, Y. Tan, and C. Su, "Generalized Prandtl-Ishlinskii Hysteresis: Modeling and Robust Control for Smart Actuators", *48th IEEE Conference on Decision and Control*, 2009, pp. 7279-7284.

[8] C. Jiang, M. Deng, and A. Inoue, "Robust stability of nonlinear plants with a non-symmetric Prandtl-Ishlinskii hysteresis model", *International Journal of Automation and Computing*, vol. 7, 2010, pp. 213-218.

[9] J. Fu, W. Xie, and S. Wang, "Robust adaptive control of a class of nonlinear systems with unknown Prandtl-Ishilinskii-Like hysteresis", *CDC/CCC 2009 Proceedings of the 48th IEEE Conference on Decision and Control and 28th Chinese Control Conference*, 2009, pp. 2448-2453.

[10] Q. Wang, C. Su, and X. Chen, "Robust adaptive control of a class of nonlinear systems with Prandtl-Ishlinskii hysteresis", *43rd IEEE Conference on Decision and Control,* 2004, pp. 213-218.

[11] C. Su, Q. Wang, X. Chen, and S. Rakheja, "Adaptive variable structure control of a class of nonlinear systems with unknown Prandtl–Ishlinskii hysteresis", *IEEE Transactions on Automatic Control*, 2005, pp. 2069.

[12] S. Bashash and N. Jalili, "Robust Multiple Frequency Trajectory Tracking Control of Piezoelectrically Driven Micro/Nanopositioning Systems", *IEEE Transactions on Control Systems Technology*, vol. 15, 2007, pp. 867-878.

[13] J. Shen, W. Jywe, H. Chiang, and Y. Shu, "Precision tracking control of a piezoelectric-actuated system", *Precision Engineering*, vol. 32, 2008, pp. 71-78.

[14] K. Kuhnen, "Modeling, Identification and Compensation of Complex Hysteretic Nonlinearities: A Modified Prandtl - Ishlinskii Approach", *European Journal of Control*, vol. 9, 2003, pp. 407-418.

[15] K. Kuhnen and P. Krejci, "Identification of Linear Error-Models with Projected Dynamical Systems", *Mathematical and Computer Modelling of Dynamical Systems*, vol. 10, 2004, pp. 59–91.

[16] M. Polycarpou, J. Farrell, and M. Sharma, "On-line approximation control of uncertain nonlinear systems: issues with control input saturation", *Proceedings of the 2003 American Control Conference,* , 2003, pp. 543-548.